Solid Earth Discuss., 4, 1511–1544, 2012
www.solid-earth-discuss.net/4/1511/2012/
doi:10.5194/sed-4-1511-2012

Solid Earth Discussions

Influence of a component of solar irradiance on radon signals at 1 km depth, Gran Sasso, Italy

G. Steinitz[1], **O. Piatibratova**[1], **and N. Charit-Yaari**[2]

[1]Geological Survey of Israel, Jerusalem, Israel
[2]MadaTech Israel National Museum of Science, Technology and Space, Daniel and Matilde Recanati Center (ra), Haifa, Israel

Received: 4 November 2012 – Accepted: 10 December 2012 – Published: 14 December 2012

Correspondence to: G. Steinitz (Steinitz@gsi.gov.il), O. Piatibratova (Oksana@gsi.gov.il), N. Charit-Yaari (naamagy@gmail.com)

Published by Copernicus Publications on behalf of the European Geosciences Union.

Abstract

Exploratory monitoring of radon is conducted at one location at the deep underground Gran Sasso National Laboratory (LNGS). Measurements (15-min resolution) are performed over a time span of ca. 600 days in the air of the surrounding calcareous country rock. Utilizing both alpha and gamma-ray detectors systematic and recurring radon signals are recorded. Two primary signal types are determined: (a) non-periodic Multi-Day (MD) signals lasting 2–10 days, and (b) Daily Radon (DR) signals – which are of a periodic nature exhibiting a primary 24-h cycle. The local ancillary environmental conditions (P, T) seem not to affect radon in air monitored at the site. Long term patterns of day-time measurements are different from the pattern of night-time measurements indicating a day-night modulation of gamma radiation from radon in air. The phenomenology of the MD and DR signals is similar to situations encountered at other locations where radon is monitored with a high time resolution in geogas at upper crustal levels. In accordance with recent field and experimental results it is suggested that a components of solar irradiance is affecting the radiation from radon in air, and this influence is further modulated by the diurnal rotation of Earth. The occurrence of these radon signals in the 1 km deep low radiation underground geological environment of LNGS provides new information on the time variation of the local radiation environment. The observations and results place the LNGS facility as a high priority location for performing advanced investigations of these geophysical phenomena, due to its location and its infrastructure.

1 Introduction

Radon (^{222}Rn) is a radioactive inert gas formed by disintegration from ^{226}Ra as part of the ^{238}U decay series. The combination of its noble gas character and its radioactive decay makes it a unique ultra-trace component for tracking temporally varying natural processes in subsurface systems.

SED

4, 1511–1544, 2012

Influence of a component of solar irradiance on radon signals at 1 km depth

G. Steinitz et al.

Numerous works have dealt with radon variations in the subsurface geological environment. Large temporal variations of radon are often encountered in air in the geologic environment, at time scales from diurnal to annual. Interpretations as to the nature of these variations, unique to Rn, often invoke either above surface atmospheric variations, or the influence of subtle active geodynamic processes. It is assumed that the temporal patterns of Rn in the geogas phase are due to processes affecting its exhalation from the country rock and/or gas transfer processes in the complex consisting of rock porosity and subsurface air space. Environmental influences, particularly atmospheric pressure and temperature, have been proposed for the origin of the periodic signals observed in Rn time series (Shapiro et al., 1985; Ball et al., 1991; Pinault and Baubron, 1997; Finkelstein et al., 2006). However, other studies indicate that a consistent meteorological influence cannot be identified as giving rise to variability in Rn time series, and suggest gravitational tides as an influencing factor on Rn variability (Aumento 2002; Groves-Kirby et al., 2006; Crockett et al., 2006, Weinlich et al., 2006; Alekseenko et al., 2009). Despite the presumed advantages of Rn as a geophysical proxy, understanding of the origin of the different Rn signals remains a challenging task.

The occurrence of radon signals has also been observed at considerable depth, at sites which are within rock systems. At these levels the air pressure regime is related to the local atmospheric barometric pressure while temperature tends to show stabile patterns reflecting the rock temperature at depth. Radon signals characterized by systematical recurrence of patterns in the temporal, geologic and geographic domains have been reported from tunnels and boreholes in France (Trique et al., 1999), from Tenerife to a depth of >800 m (Martin, 1999; Martin et al., 2002; Eff-Darwich et al., 2002) and from the desert in Israel to a depth of >100 m (Barbosa et al., 2010; Steinitz et al., 2007; Steinitz and Piatibratova, 2010a, b).

The setting of Laboratori Nazionali Gran Sasso (LNGS) offers a unique opportunity to investigate the temporal signals due to a combination of qualities: (a) underground, at a depth in the order of 1000 m; (b) low background radiation environment. First radon

SED
4, 1511–1544, 2012

measurements and monitoring results in air and the local hydrologic system of LNGS were reported by Bella and Plastino (2000) and Plastino and Bella (2001). This contribution describes patterns and characteristics of radon signals in air of the immediate surrounding country rock of LNGS. Site parameters and the unsuccessful outcome of an examination as to the influence of local environmental parameters combined with the identification of further exceptional geophysical characteristics in the time series lead us to suggest again the influence of a component in solar irradiance as a driver of radon variation.

2 Experimental setup

The underground facilities are located in a side tunnel of the ten kilometers long freeway tunnel crossing the Gran Sasso Mountain ridge from L'Aquila to Teramo. The mountain ridge towering above the laboratory results in an average depth of 1400 m of the laboratory. The laboratory is built within a thick sequence of folded and faulted Mesozoic to Tertiary sedimentary units of the Gran Sasso massif in the central Apennines (Ghiseti, 1987). The LNGS facility is excavated in limestone and dolomite with ^{238}U activities in the range of 0.42 to 6.8 ppm (Wulandary et al., 2004). The hydrological situation is such that the laboratory is situated below the regional water table. The facility consists of three large experimental halls, each about 100 m long, 20 m wide and 18 m high and interconnecting service tunnels. The tunnels and rooms of the LNGS facility are lined with concrete walls (60 cm thick), serving as a shield for the laboratory – mechanical, hydrologic and environmental radiation (Bettini, 2000). Radon measurements in experiment halls with concrete lining are in the range of 20–150 kBq m^{-3}, depending on the ventilation regime (Bassignani et al., 1997).

Radon monitoring is performed in a side room, roughly 4 × 2 × 2 m, along one of the service tunnels of the facility (Fig. 1). The country rock, composed of steeply dipping beds of limestone and marl, is exposed at the side walls and ceiling of the site. The room is separated from the service tunnels by a metal partition and tight door (both fitted with a rubber seal), limiting the exchange of air in the room with air in the service tunnel, while allowing a good contact with air of the surrounding country rock.

Radon measurements are performed utilizing alpha and gamma-ray detectors. Utilization of gamma detector systems for monitoring Rn is based on the detection of gamma radiation from the ^{214}Bi and ^{214}Pb. Due to the short half lives of the Rn daughters equilibrium of the Rn and its daughters is achieved after a short time ($\sim$ 100 min). Two $2'' \times 2''$ NaI detectors fitted with a single channel analyzer in the range of 50–3000 keV (PM-11 detector, ROTEM Inc., Israel) are placed in parallel and horizontally at the monitoring site to record the gamma radiation emitted from the walls and from radon in the air of the room. The advantages of using these detectors for monitoring of radiation from radon is given by Zafrir et al. (2011). Varying radon levels are recorded by the count rate of the gamma detectors, connected to a datalogger. The direct measurement of radon by alpha radiation is performed with a calibrated Alphaguard system (Genitron Gmbh). Ancillary environmental parameters (P, T, RH) are recorded by the Alphaguard system in the initial phase and ongoing P and T monitoring was installed in November 2006. Integration times are set to 15 min for the gamma system and 10 min for the alpha system. The elapsed time is shown on a decimal-day scale (relative to zero day at 1 January 2005).

The bulk of the results rely on data obtained using two PM-11 gamma sensors operated in tandem during more than 500 days (Fig. 2). The Alphaguard system was operated during an initial stage and also for several intervals in parallel to the gamma detectors. The temporal variation of radon recorded by the gamma detectors was pre-processed in the following manner:

1. The observations in the time series of the two gamma sensors were summed as one gamma sensor with an improved sensitivity.

2. The resulting time series was smoothed utilizing a 25-h sliding average. Such a decomposition of the time series highlights the different signals contained in it.

SED
4, 1511–1544, 2012

3. The residual time-series was de-noised using a further 9-sample sliding average in order to emphasize some aspects.

3 Results

The main results of the alpha signal of radon variation and ancillary parameters in the air of the site obtained in the initial stage are shown in Fig. 3. Upon the closing of the site door the following features are observed:

1. A fast decrease of temperature from a level of 17–18 °C to a stable level around 11.5 °C with a variation less than ±0.3 °C.

2. A parallel increase in humidity to a stable level of around 93 %.

3. A time varying pressure.

4. A rapid and significant buildup of radon from around 100 Bq m^{-3} to around 450 Bq m^{-3} followed by temporal variation.

The new conditions at the site are attained within two days after isolating the site from the laboratory atmosphere and environment. The attained overall radon level of around 400 Bq m^{-3} is relatively low compared with most subsurface geogas in geological environments. Monitoring results (around 40 days) show that the temperature and humidity levels are very stable over time. Small variations in temperature (<0.5 °C) are probably reflecting temperature variations in the adjoining service tunnel. The temporal pattern of radon indicates the occurrence of daily and multi-day signals, which vary following a pattern that differs from those of pressure and temperature.

Figure 4 shows the temporal variation of radon measurement with alpha detector (AlphaGuard system) and the simultaneous record from the two gamma detectors. The two gamma detectors exhibit very similar variation patterns which are parallel to the alpha signal. Measurements using the two gamma sensors and the alpha detector are instrumentally independent. Thus operation of the Alphaguard system in parallel with the gamma detectors substantiates that the variation in the gamma radiation represents variation of radon in the air of the room. The recorded gamma radiation originated from two sources: (a) a constant component due to the radioactive elements in the wall rock (and concrete), and (b) a varying component emitted from radon decay products in the air of the site. The count rate of both gamma sensors is similar, and the systematic difference among them can be attributed to a slight difference in sensitivity and/or due to their slightly differing positions. The higher count rate of the gamma sensor, relative to the alpha detector, reflects the large difference of the sampled volume (due to the different range of alpha and gamma radiation in air; see also Zafrir et al., 2011). The high correspondence of the radiation pattern recorded by the two gamma sensors allows referring to them as a single detector by summing the two count rates, thus improving the signal to noise ratio.

Taking into consideration the complete data set, systematic temporal variations in the radon level are observed. The primary variation is manifested as signals lasting one to several days. A very high concordance is observed among the time series of these detectors (Fig. 4a), which is enhanced by de-noising each time series using a 9-point sliding average (Fig. 4b). This concordance enables the following conclusions:

1. The radon concentration in the room air varies in a systematic pattern.

2. Variations in the order of 50 Bq m^{-3} (alpha sensor) and around 500 counts/15-min are above the statistical uncertainty and reflect variations due to environmental and/or geophysical processes.

Two types of signals occur in the radon time series – Daily Radon (DR) signals and Multi-Day (MD) signals, similar to those encountered in several other sites and locations (Steinitz et al., 2007). The MD signals, with amplitudes of over 10 kcounts/15-min, span two or more days and are non-periodic. A typical representation of the MD signal is given in Fig. 5 using the smoothed time series showing that they have both symmetric and asymmetric forms.

SED
4, 1511–1544, 2012

The DR signal occurs as a periodic signal but with highly irregularly varying daily amplitude (Fig. 6). In some days it appears as if a minor semi-diurnal component is also present in the time series. Generally no relation can be determined between the MD and DR signals (Fig. 6a), but in some time intervals, lasting several tens of days, an apparent relation is observable (Fig. 6b).

Further insight into the DR signal is gained by spectral analysis. FFT spectrum was calculated for the combined gamma time series for 222 days - the longest continuous data set available (Days 403–625). In order to enable a long time series a jump in the background level, occurring at 565.6, was rectified by adjusting the following data to the previous ones. To this end 10-day long averages were calculated prior to and following the offset, and the difference (= 206.6 counts/15-min) was used to adjust the subsequent data. Linear detrending was applied to the data set in the course of the FFT analysis.

The FFT results (Fig. 7) shows that a small but well distinguished diurnal constituent occurs in the data set. The primary diurnal cyclic constituent (= 0.99997 cycles day^{-1}) represents a frequency of one cycle day^{-1}. The occurrence of a further semi-diurnal constituent with a frequency of two cycles day^{-1} is also apparent in Fig. 7. The observation of a semi-diurnal periodicity in this time series suggests that this frequency may represent a geophysical feature.

Concurrent environmental parameters measured at the radon monitoring site include temperature, humidity and air pressure. Humidity and temperature show very stable patterns. Pressure shows a multi-day variation, a generally well known pattern. The latter is affected by ventilation driving fresh air from the surface outside the LNGS which dilutes the indoor radon due to its low level. Radon level at the monitoring site reflects primarily the content of radon in the air of the country rock adjacent to the laboratory.

In numerous cases it is reported that variation patterns in radon time series seem at first hand to reflect an atmospheric – pressure and/or temperature – driving mechanism. Temperature at the measurement site is stable (Fig. 3). The plot in Fig. 8 demonstrates the temporal variation of gamma radiation from radon with the variation

SED
4, 1511–1544, 2012

of pressure measured both at the subsurface site and at the above surface. The pressure in the lab follows the surface pressure, but it is probably somewhat affected by the ventilation system. The gamma radiation pattern follows a different pattern. Different time intervals show both similar and dissimilar co-variation patterns among pressure and gamma radiation. Simultaneous measurement of pressure and radon by the Alphaguard system allows a comparison of the radon level and the local air pressure. Figure 9 shows the relations between the radon level versus the indoor air pressure (Fig. 9a) and the relation between the gradients of pressure and radon (Fig. 9b). The apparent absence of correlation, particularly between radon values and pressure gradient, suggests that pressure variations cannot be considered as a straightforward and direct driver of the radon variation at the confined conditions of the site.

Time series of atmospheric pressure measurements typically contain diurnal (24-h cycle) and semidiurnal (12-h) periodic variations (Richon et al., 2009), with relative amplitudes that change from place to place and in time. This allows also investigating the eventual connection between radon and pressure in the frequency domain. Using the data from day 668 onwards (November 2006) the spectra of radon and pressure at the monitoring site are shown in Fig. 10. The resulting spectra indicate that a 24-h periodic constituent is observed in the radon signal while no such cycle is observed in the pressure. It can thus be assumed that the observed variation in pressure at the site is reflecting the pressure regime in the underground laboratory.

The long term variation in the frequency-time domain of subsurface pressure and radon were analyzed using the Continuous Wavelet Transform (CWT). Different patterns of variation are observed (Fig. 11). The variation of pressure in the frequency-time domain is uniform. In comparison the variation of radon is irregular in the same frequency-time domain. This is indicating, again, that variation of pressure is not driving the variation in radon.

An advanced re-analysis (Sturrock et al., 2012) of the gamma radiation from the primary radon in air experiment of Steinitz et al. (2011) demonstrated, among other things, that different temporal variation patterns occur depending on whether day-time

SED
4, 1511–1544, 2012

or night-time measurements are considered. The existence of this feature in the LNGS data was investigated by applying a similar approach using the normalized hourly gamma-ray time series and performing two analysis steps:

1. The time series was decomposed to into two time series of (a) day-time (08:00–16:00 UTC) measurements, and (b) night-time (20:00–04:00 UTC) measurements. The ensuing gaps in these time series were filled by linear interpolation. Figure 12 (right) shows a CWT (Morlet wavelet) analysis of the decomposed gamma-ray time series, presented as a time-integrated-power-spectrum. Different patterns are obtained for the day-time and night-time measurements. On the other hand, the same kind of analysis performed on the decomposed time series of pressure (Fig. 12 left) results in similar and uniform patterns both for the day-time and for the night–time measurements, as is expected.

2. The 24-h periodic component in the time series was filtered and reconstructed (FFT; Fig. 13). The reconstructed time series is composed of 24 values per each day. This allows tracking per Hour-in-Day (HID) values over the whole time interval. In other words one is observing the long-term variation pattern of measurements taken at a specific hour within the daily cycle. Using such a measurement scheme (a specific hour in each day) the anticipation is that no systematic pattern occurs. Figure 14 shows the decomposed set of 24 HID time series showing that in difference with the expected the time series vary in a regular interwoven pattern. Further examination shows that this internal HID structure of the S1 periodic component is actually composed of 12-pairs of inverse time series with a twelve hour difference per pair. Figure 15 presents two examples of such pairs. The overall pattern of the HID variation is presented as a 3-D diagram in Fig. 14 showing that the normalized level of the 24-h component is strongly positive around 04:00 UTC and highly negative 12 h later, around 16:00 UTC.

The results of both analyses indicate that a day-night differentiation occurs in the gamma radiation from radon at LNGS, similar to that observed by Sturrock et al. (2012).

SED
4, 1511–1544, 2012

Furthermore, the 12-h asymmetry indicates that this feature is connected to the rotation of Earth around its axis.

4 Discussion and conclusions

The concordant radon signal measured utilizing two independent radiation detector systems confirms the exactness of the absolute radon content and its variation in the air inside the monitoring site, which is in contact with the geogas system of the locally exposed rock face. The overall environmental features of the measurement site limit the option of mass transfer to explain the variations in radon. Radon originates in the surrounding rock system from where it diffuses into the experiment room. The level of radon in the adjacent rock porosity and crevices is certainly higher than that in the experiment room and thus does not constitute a sink for radon. Fast decrease of the level of radon in the order of 10 % within a day occurs from time to time. Such a decrease cannot be accounted for by mass transfer out of the room. The tightness of the room and the stable temperature and humidity patterns in the room indicate that there is no significant exchange of air mass between the room and the laboratory, especially at a daily scale. Furthermore, there is no reason to assume selective transfer of radon from the air in the room.

Two types of signals occur in the temporal variation pattern of radon in the geogas at LNGS – a non-periodic multi day (MD) signal and a diurnal radon (DR) signal. The periodic character of the DR signal enables a deeper insight and a further comparison of characteristics with those of local environmental parameters. Local temperature, governed by the surrounding rock temperature, is apparently not related to the variation of radon as it is very stable. Pressure gradient is often raised as a driver of radon variation in geogas. Analysis for correlation in the time-, frequency- and frequency-time domains shows that temporal variation of radon is not

directly and simply related to the variation of pressure. This situation indicates that variation of air pressure also cannot be considered as the primary driver of the cyclic

SED
4, 1511–1544, 2012

DR signals, and probably also not of further components of the radon variation. In turn this implies that a different periodic process is operating which produces the 24-h cyclic variation in the radon signal.

The processes driving the radon signals in air at LNGS are not defined at this stage. The following features and considerations may shed light on these processes:

1. Incompatibility of above surface atmospheric processes – both temperature and pressure – as primary driving mechanisms.

2. A clearly defined non-periodic MD signal occurs in the radon time series of LNGS. Elsewhere (Steinitz et al., 2003) such signals have been associated with subtle geodynamic transients affecting the local rock system, based mainly on a statistical correlation of such signals with earthquakes in a geologically related domain. Determining a connection between radon emission and active geodynamics is not possible due to lack of information on the spatial distribution of such signals around LNGS.

3. The periodic DR signal at LNGS is not influenced by solid earth gravity tide processes. The main diurnal constituent is only a 24-h period (S1), whereas the constituents typical for gravitational interaction (primarily M2; Wilhelm et al., 1997) are lacking. This probably indicates that the weak tidal-mechanical effects are not influencing the radon signal. Similar conclusions are arrived at from recent investigations at other locations (see below).

4. The apparent partial association between the multi-day signal and the amplitude of the diurnal variation (peak-to-peak) opens the possibility for some sort of coupling.

5. A long term difference among day-time and night-time measurements is observed, a feature which is not known for other geophysical time series (atmospheric, solid earth).

SED
4, 1511–1544, 2012

Radon signals in geogas within rock systems in upper crustal levels have been intensely studied in Israel (Steinitz et al., 1999, 2003, 2006) and Tenerife (Gazit-Yaari and Steinitz, 2003; Steinitz et al., 2006). Geophysical analysis of these relatively long time series measured with a high time resolution (within 1 h) demonstrate that Rn signals in air confined within rock units are characterized by systematical recurrence of signal patterns in the temporal, geologic and geographic domains, to depth of > 100 m. The main types recognized are multi-year, annual-radon (AR; periodic), multi-day (MD) and daily-radon (DR; periodic) signals (Steinitz et al., 1992; Steinitz et al., 1999, 2007; Barbosa et al., 2010) as well as intense variation lasting several hours (Steinitz and Piatibratova, 2010a, b). Examination of the patterns suggested that:

1. Variation patterns in the subsurface regime cannot be accounted for by simple and direct time varying processes in the gas system such as emanation, diffusion, absorption and advection;

2. Absence of above surface atmospheric influence, in particular pressure.

3. Periodicity in the DR signal is characterized by solar periodicities, implying an external above surface driving mechanism;

Based on the accumulated data and phenomenology it was suggested that a component of solar irradiance is influencing the radon signal, primarily the periodic signals. Further insight on the issue was recently gained by experimental simulation of radon signals in confined volumes of air (Steinitz et al., 2011). In contrast to the expectation the results demonstrate nuclear radiation patterns that are non uniform in space and in time. The variations (20 %) were both periodic and non-periodic, spanning several orders of temporal magnitude – from annual to daily. The results, obtained under static and isolated conditions, are in disagreement with the expected radioactive equilibrium and its spatially uniform expression within and around the experimental volume. The characteristics of the prominent periodic signals indicate forcing by a component of solar tide which can traverse 5 cm of lead. These experimental results are in line with the

SED

4, 1511–1544, 2012

observations from the geological environment, and conform to the implied geophysical consequences. Reanalysis by Sturrock et al. (2012) of the long experimental radon time series could: (a) corroborate the results;(b) present evidence of solar rotational frequencies (which are independent of Earth) in the nuclear radiation time series, and (c) show a 24-h modulation of the gamma radiation of the radon system in the annual and solar frequency bands. In conformity with the view in previous works Sturrock et al. (2012) suggested that the decay is influenced by solar radiation and solar neutrinos were considered as a possible particle involved.

The radon signals observed within confined air of the rock system at NLGS, at 1 km depth, show similarities with the observations in the above works – in terms of the radon patterns and the dilemmas versus eventual atmospheric drivers. Therefore it is suggested that other geophysical processes drive the nuclear radiation from radon at LNGS. If this is the case then the possibility is raised that the driver of the daily periodic component at LNGS is also due to a component of solar irradiance. The occurrence of a day/night difference in the DR signal at LNGS supports the notion that solar irradiance is influencing the nuclear radiation from radon in air. The day/night effect is a modulation of this influence due to the rotation of Earth around its axis.

Identification of geophysical radon signals in the air in the realm of Gran Sasso has specific implications for research in this field and on related subjects, as follows:

1. The occurrence of such geophysical signals in a further geographic location (central Apennines).

2. Observing such phenomena in a calcareous sequence with a low uranium content.

3. The phenomena are detected at a depth in the order of 1000 m below the surface.

4. Observing radon signals at a level situated below the regional water table.

5. Providing new information on the environmental radiation phenomena at LNGS, including aspects of its local specific temporal variation.

SED
4, 1511–1544, 2012

6. Setting ground for the exceptional option of performing advanced physical and geophysical investigations on the radon system based on the infrastructure of LNGS.

The observations and results mark the LNGS facility as a high priority location for performing advanced investigations of geophysical phenomena of the radon system, due to its location and its infrastructure (Bettini, 2000; Bella and Plastino, 2000; Plastino and Bella, 2001; Plastino et al., 2001, 2007; Plastino, 2006). The present investigation was hampered by the combination of the overall low radon signal and the limitations imposed by the analytical system employed. To overcome this situation and to explore the remaining questions such as to the influence of local environmental influences controlled active experiments as devised and described by Steinitz et al. (2011) should be performed at deep underground laboratories such as LNGS (IT) and LSC (ES).

Acknowledgements. This activity was performed in the frame of ILIAS-TARI project ERMES-Radon at LNGS (P2005-02-LNGS). The project is also supported (to GS) by Israel Science Foundation grant ISF 524/05.

W. Plastino enabled and provided support for this activity. G. De Luca helped with the installation and running the measurements. Uri Malik prepared the analytical gamma system and G. Haquin helped in the initial stage of the activity..

References

Alekseenko, V. V., Gavriluk, Y. M., Kuziminov, V. V., and Stenkin, Y. V.: Tidal effect in radon-due neutron flux from the Earth's crust, J. Phys.: Conf. Ser. 203, 012045, doi:10.1088/1742-6596/203/1/012045, 2009.

Aumento, F.: Radon tides on an active volcanic island: Terceira, Azore, Geofísica Internacional, 41, 499–505, 2002.

Bassignani, A., Bam, B. B., Colombo, G., Fresca Fantoni, R., Giacomelli, G., Mascoli, M., Fracchetta, V., Patrizii, L., and Sartorio, C.: Measurements of radon concentration and gamma ray activity in Hall B of the Gran Sasso Laboratory, Radiat. Meas., 28, 609–612, 1997.

SED

4, 1511–1544, 2012

Barbosa, S. M., Zafrir, H., Malik, U., and Piatibratova, O.: Multi-year to daily Radon variability from continuous monitoring at the Amram tunnel, southern Israel, Geophys J., Int. 182, 829–842, doi:10.1111/j.1365-246X.2010.04860.x, 2010.

Ball, T. K., Cameron, D. G., Colma, T. B., and Roberts, P. D.: Behavior of radon in the geological environment: a review, Q. J. Eng. Geol., 24, 169–182, 1991.

Bella, F. and Plastino, W.: Radon time series analysis at Laboratori Nazionali del Gran Sasso, II, Laboratori Nazionali del Gran Sasso – I.N.F.N., Annual Report 1999, 199-203, 2000.

Bettini, A.: A Vision Becomes Reality. The Gran Sasso Laboratory 1979–1999, Instituto Nazionale di Fisica Nucleare Ed., 304 pp., 2000.

Crockett, R. G. M., Gillmore, G. K., Phillips, P. S., Denman, A. R., and Groves-Kirby, C. J.: Tidal synchronicity of built-environment radon levels in the UK, Geophys. Res. Lett., 33, L05308, doi:10.1029/2005GL024950, 2006.

Eff-Darwich, A., Martin-Luis, C., Quesada, M., delaNuez, J., and Coello, J.: Variations on the concentration of ^{222}Rn in the subsurface of the volcanic island of Tenerife, Canary Islands, Geophys. Res. Lett., 29, 26–29, 2002.

Finkelstein, M., Eppelbaum, L. V., and Price, C.: Analysis of temperature influences on the amplitude frequency characteristics of radongas concentration, J. Environ. Rad., 86, 251–270, 2006.

Gazit-Yaari, N. and Steinitz, G.: Project TeRn – Activity report, March 2002 – February 2003, Isr. Geol. Surv. Rep. TR-GSI/5/03, 55 pp., 2003.

Ghiseti, F.: Mechanism of thrust faulting in the Gran Sasso chain (central Apennines, Italy), J. Struct. Geol., 9, 955–966, 1987.

Groves-Kirby, C. J., Denman, A. R., Crockett, R. G., Phillips, P. S., and Gillmore, G. K.: Identification of tidal and climatic influences within domestic radon time series from Northamptonshire, UK, Science of the Total Environ., 367, 191–202, 2006.

Martin, M. C.: Variacion espacio – temporal del nivel de emision de radon en una zona volcanica activa: Tenerife (Islas Canarias), Ph.D. thesis, University of La Laguna, de La Laguna, 270 pp., 1999.

Martin, C., Quesada, M. L., Eff-Darwich, A., De la Nuez, J., Coello, J., Ahijado, A., Casillas, R., and Soler, V.: A new strategy to measure radon in an active volcanic island (Tenerife Canary Islands), Environ. Geol., 43, 72–78, 2002.

Pinault, J. L. and Baubron, J. C.: Signal processing of diurnal and semidiurnal variations in Radon and atmospheric pressure: a new tool for accurate in situ measurement of soil gas velocity, pressure gradient, and tortuosity, J. Geophys. Res., 102, 18101–18120, 1997.

Plastino, W.: Monitoring of geochemical and geophysical parameters in the Gran Sasso aquifer, Radionuclides in the Environment, Elsevier, 335–342, 2006.

Plastino, W. and Bella, F.: Radon groundwater monitoring at underground laboratories of Gran Sasso (Italy), Geoph. Res. Lett., 28, 2675–2677, 2001.

Plastino, W., Kaihola, L., Bartolomei, P., and Bella, F.: Cosmic background reduction in the radiocarbon measurements by liquid scintillation spectrometry at the underground laboratory of Gran Sasso, Radiocarbon, 43, 157–161, 2001.

Plastino, W., Chereji, I., Cuna, S., De Felice, P., Kaihola, L., Lupsa, N., Balas, G., Mirel, V., Berdea, P., and Baciu, C.: Tritium in water electrolytic enrichment and liquid scintillation counting, Radiat. Meas., 42, 68–73, 2007.

Richon, P., Perrier, F., Pili, E., and Sabroux, J. C.: Detectability and significance of 12 h barometric tide in radon-222 signal, dripwater flow rate, air temperature and carbon dioxide concentration in an underground tunnel, Geophys. J. Int., 176, 683–694, 2009.

Shapiro, M. H., Rice, A., Mendenhall, M. H., Melvin, J. D., and Tombrello, T. A.: Recognition of environmentally caused variations in Radon time series, Pure Appl. Geophys., 122, 311–326, 1985.

Steinitz, G. and Piatibratova, O.: Radon signals in the Gavnunim intrusion, Makhtesh Ramon, Israel, Geophys. J. Int., 180, 651–665, 2010a.

Steinitz, G. and Piatibratova, O.: Radon signals at the Roded site, Southern Israel, Solid Earth, 1, 99–109, doi:10.5194/se-1-99-2010, 2010b.

Steinitz, G., Vulkan, U., Lang, B., Gilat, A., and Zafrir, H.: Radon emanation along border faults of the Rift in the Dead Sea area, Israel J. Earth Sci., 41, 9–20, 1992.

Steinitz, G., Vulkan, U., and Lang, B.: The Radon flux at the northwestern segment of the Dead Sea (Dead Sea Rift) and its relation to earthquakes, Israel J. Earth Sci., 48, 283–299, 1999.

Steinitz, G., Begin, Z. B., and Gazit-Yaari, N.: A statistically significant relation between Rn flux and weak earthquakes in the Dead Sea rift valley, Geology, 31, 505–508, 2003.

Steinitz, G., Martín, M. C., Gazit-Yaari, N., Quesada, M. L., de la Nuez, J., Casillas, R., Malik, U., and Begin, Z. B.: Multi-day Radon signals with a radioactive decay limb – occurrence and geophysical significance, Appl. Radiat. Isotopes, 64, 520–524, doi:10.1016/j.apradiso.2005.10.004, 2006.

SED

4, 1511–1544, 2012

Steinitz, G., Piatibratova, O., and Barbosa, S. M.: Radon daily signals in the Elat Granite, southern Arava, Israel, J. Geophys. Res., 112, B10211, doi:10.1029/2006JB004817, 2007.

Steinitz, G., Piatibratova, O., and Kotlarsky, P.: Possible effect of solar tides on radon signals, J. Environ. Radioac., 102, 749–765, doi:10.1016/j.jenvrad.2011.04.002, 2011.

Sturrock, P. A., Steinitz, G., Fischbach, E., Javorsek, D., and Jenkins, J. H.: Analysis of Gamma Radiation from a Radon Source: Indications of a Solar Influence, Astropart. Phys., 36, 18–25, 2012.

Trique, M., Richon, P., Perrier, F., Avouac, J. P., and Sabroux, J. C.: Radon emanation and electric potential variations associated with transient deformation near reservoir lakes, Nature, 399, 137–141, 1999.

Weinlich, F. H., Faber, E., Bouskova, A., Horalek, J., Teschner, M., and Poggenburg, J.: Seismically induced variations in Marianske Lazne fault gas composition in the NW Bohemian swarm quake region, Czech Republic – A continuous gas monitoring, Tectonophysics, 421, 89–110, 2006.

Wilhelm, H., Zürn, W., and Wenzel H. G., (Eds.): Tidal phenomena, Lectures in Earth Sciences (Springer), 66, 1997.

Wulandari, H., Jochum J., Rau, W., and von Feilitzsch, F.: Neutron flux at the Gran Sasso underground laboratory revisited, Astropart. Phys., 22, 313–322, 2004.

Zafrir, H., Haquin, G., Malik, U., Barbosa, S. M., Piatibratova, O., and Steinitz, G.: Gamma versus Alpha Sensors for Rn-222 Long-Term Monitoring in Geological Environments, Radiat. Meas., 46, 611–620, doi:10.1016/j.radmeas.2011.04.027, 2011.

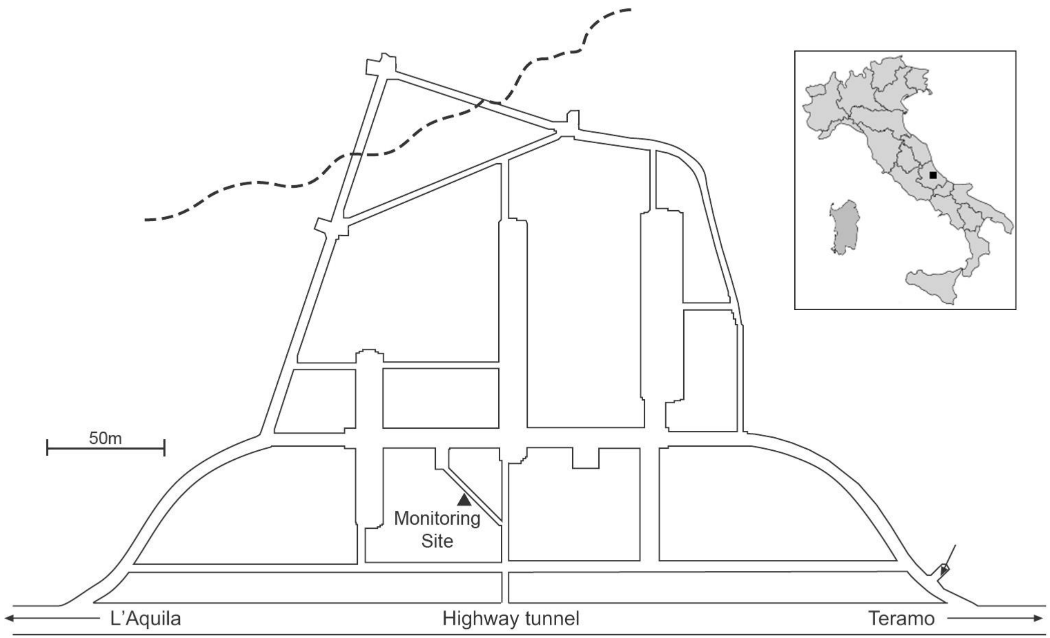

Fig. 1. Layout of LNGS underground facility. Radon measurements in air are conducted at the monitoring site which is located next to a service tunnels (hatched line – fault trace).

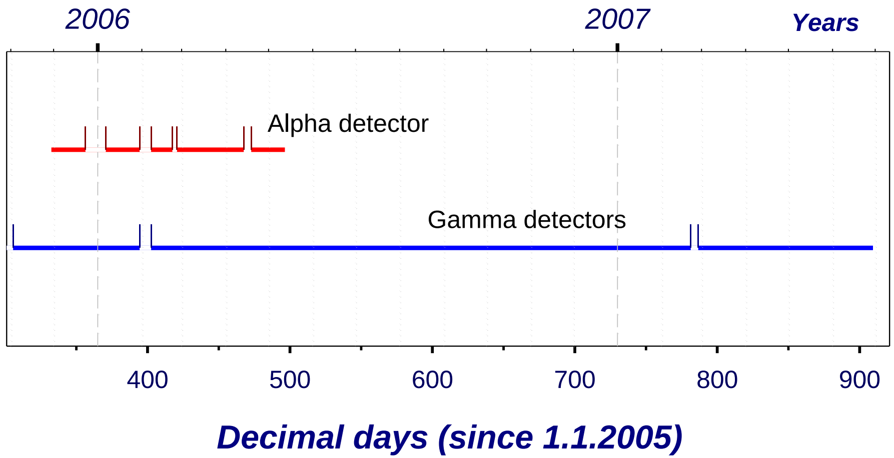

Fig. 2. Range of radon monitoring intervals using gamma detectors and co-registration with alpha detectors. Data gaps are indicated.

SED
4, 1511–1544, 2012

Influence of a component of solar irradiance on radon signals at 1 km depth

G. Steinitz et al.

Title Page
Abstract | Introduction
Conclusions | References
Tables | Figures
◀| |▶
◀ ▶
Back | Close
Full Screen / Esc
Printer-friendly Version
Interactive Discussion

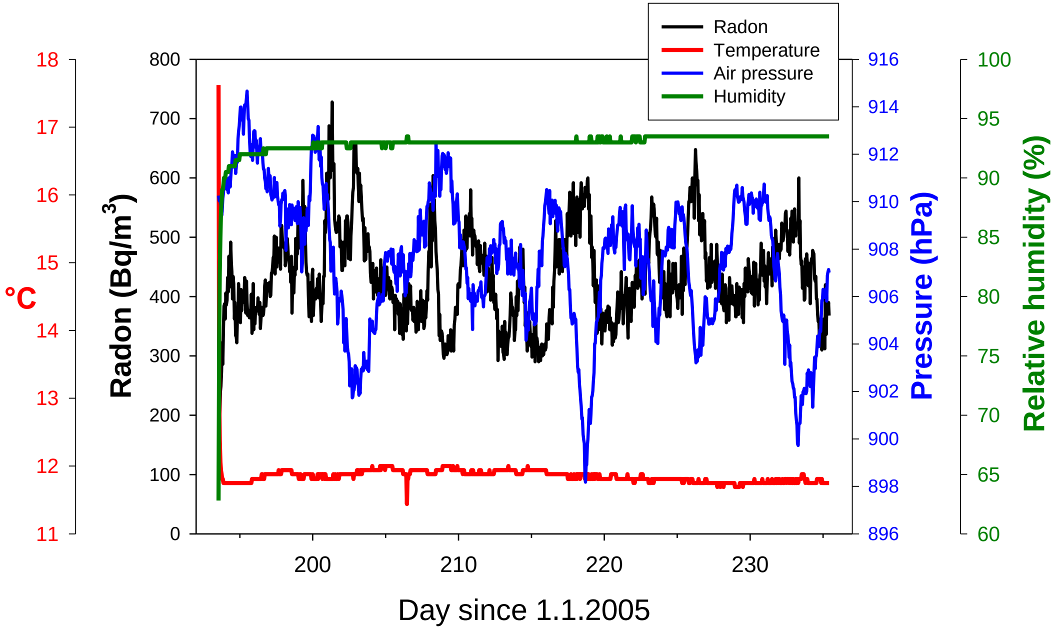

Fig. 3. Time series of radon (using an alpha detector) in air at experiment site and local environmental parameters (pressure, temperature, relative humidity).

SED

4, 1511–1544, 2012

Influence of a component of solar irradiance on radon signals at 1 km depth

G. Steinitz et al.

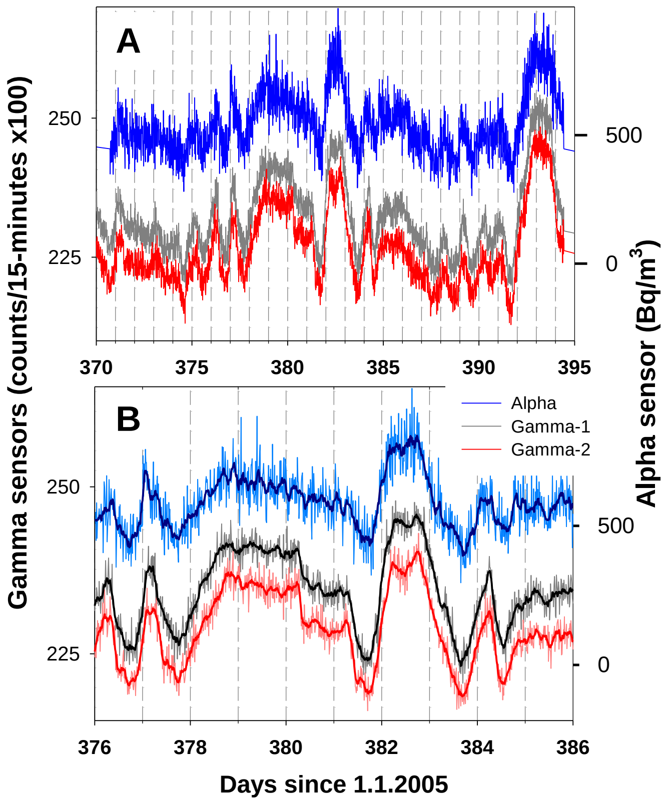

Fig. 4. (A) A 25-day interval of parallel measurements by two gamma detectors and an alpha detector displaying a high concordance of the variation. **(B)** A 10-day detail of the time series. The concordance is further manifested by de-noising each time series using a 9-point sliding average (shown as solid lines). Legend – for both figures

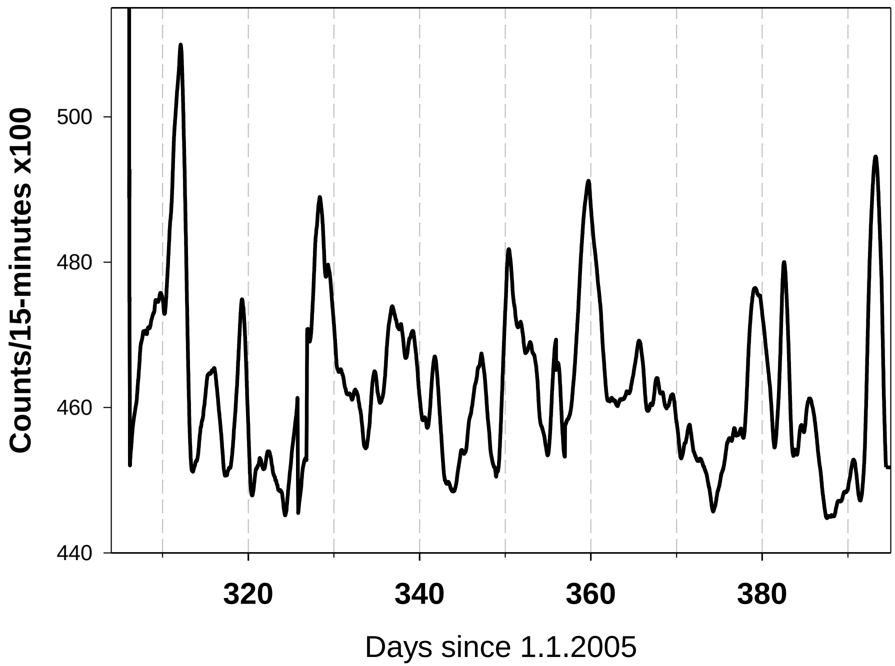

Fig. 5. A typical example of MD signals during a time interval of around 100 days. The temporal patters shown in the plot represents the combination of the signals from both of the gamma sensors (using a 25-h sliding average).

SED
4, 1511–1544, 2012

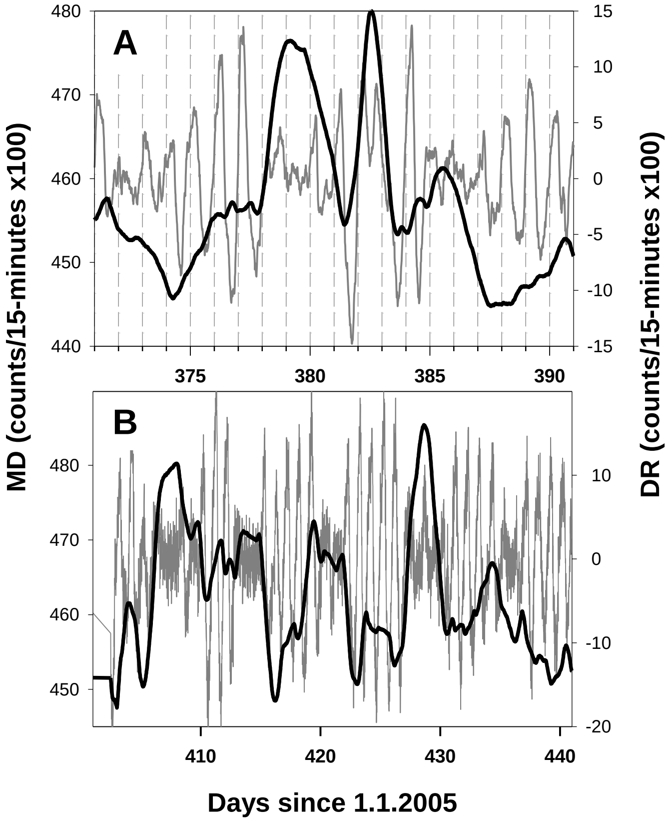

Fig. 6. Examples of relations between concurrent MD (solid) and DR (gray) signals. DR signals have been obtained after de-noising using a 9-point sliding average. **(A)** The daily amplitude of the DR signals varies in an irregular fashion. **(B)** An apparent relation is observed between the amplitude of the DR signal and the MD signal

SED
4, 1511–1544, 2012

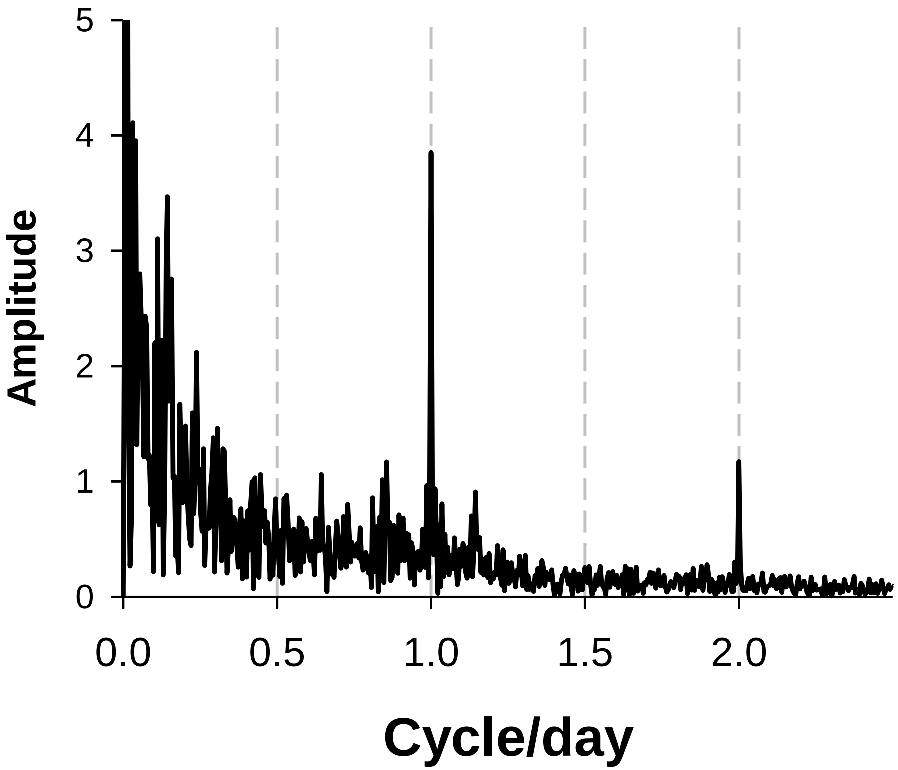

Fig. 7. FFT of the radon signal measured using the combined gamma detector signal during a 222 day period (from 564 to 776). A distinct diurnal component (1 cycle day^{-1}) is observed, and possibly also a semi-diurnal one (2 cycles day^{-1}). See text.

SED

4, 1511–1544, 2012

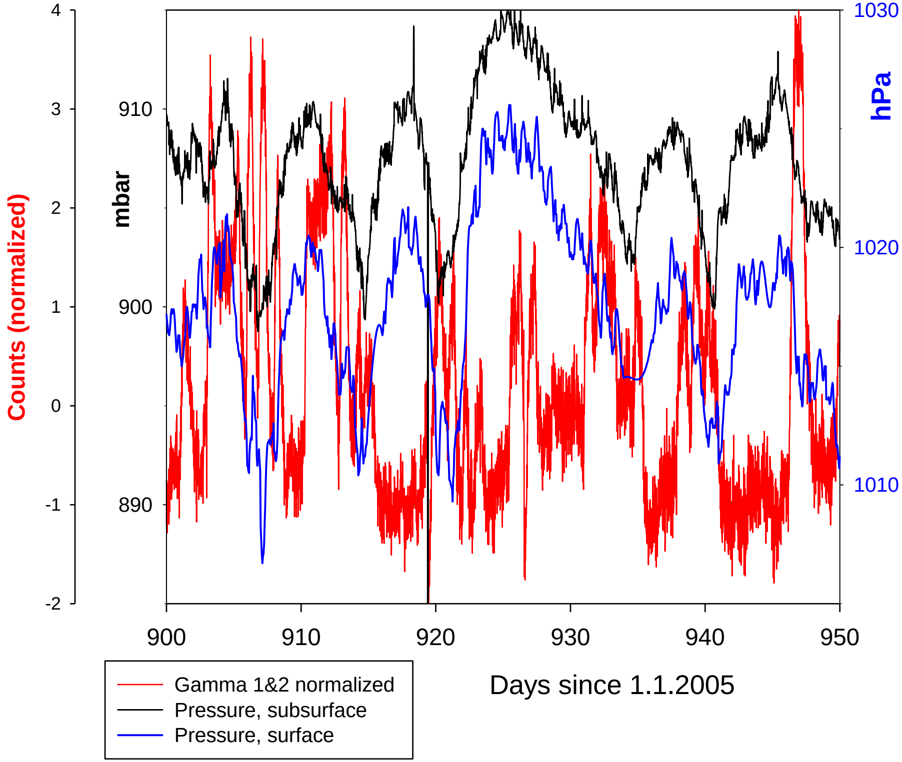

Fig. 8. Time series (50 days) of air pressure both in the subsurface lab and at surface along with concurrent variation of the gamma radiation due to radon in the air of the room. All time series are dominated by multiday signals. The subsurface pressure varies according to the above surface pressure. The variation of radon shows a different pattern.

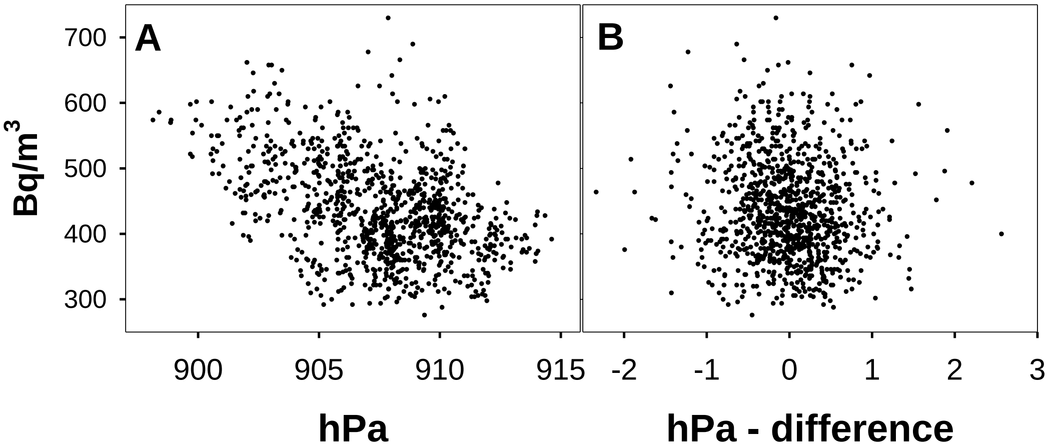

Fig. 9. Relation between: **(A)** radon level and air pressure values inside the site, and **(B)** radon difference and pressure difference between consecutive measurements. The data are hour averages of the values measured during 42 days (days 193–235) using the alpha detector system. The Pearson correlation coefficient between radon and pressure data in **(A)** is −0.442.

SED
4, 1511–1544, 2012

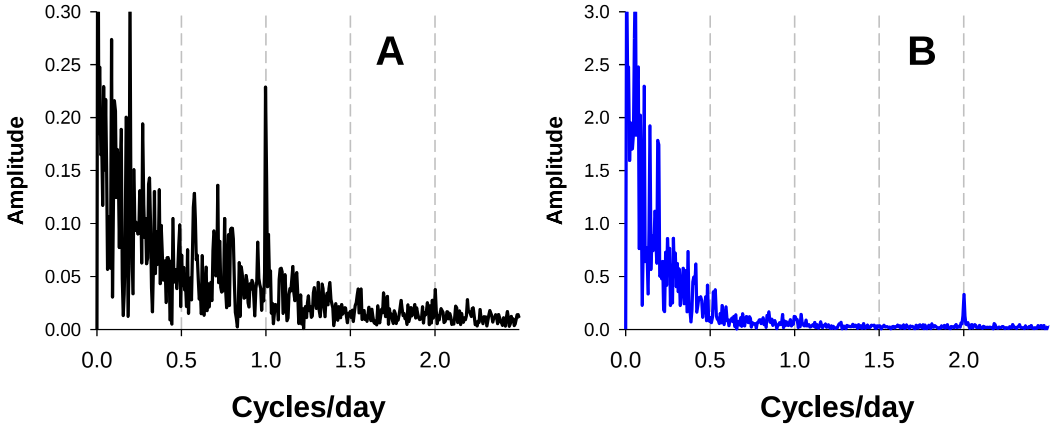

Fig. 10. Spectra (FFT) of the radon (A) and pressure (B) signals for Days 668–742, using data at a resolution of 15-min. The spectra for radon were calculated from the normalized time series. A 24-h periodic constituent is not present in the case of the pressure signal whereas it occurs in the radon signal.

SED

4, 1511–1544, 2012

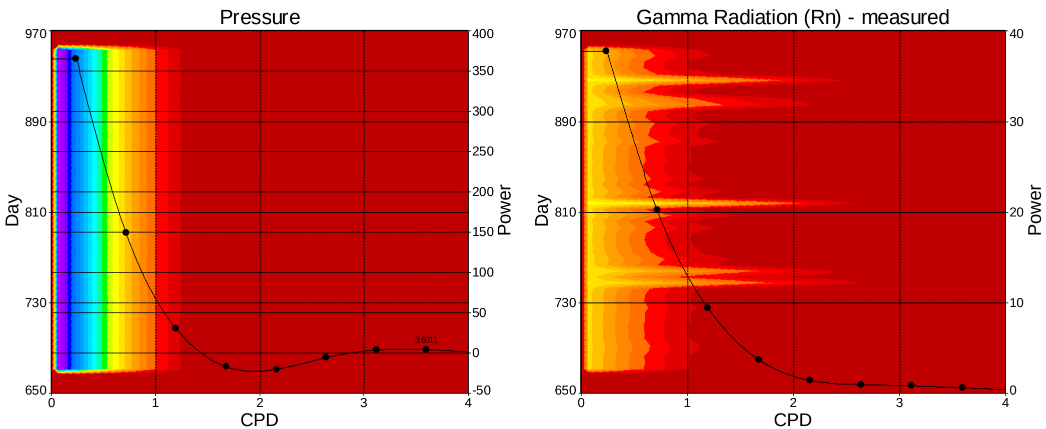

Fig. 11. CWT analysis of the site air pressure time series (left) and the normalized gamma-ray time series (right). Significantly different patterns between pressure and radon are observed in the frequency-time domain.

SED
4, 1511–1544, 2012

Influence of a component of solar irradiance on radon signals at 1 km depth

G. Steinitz et al.

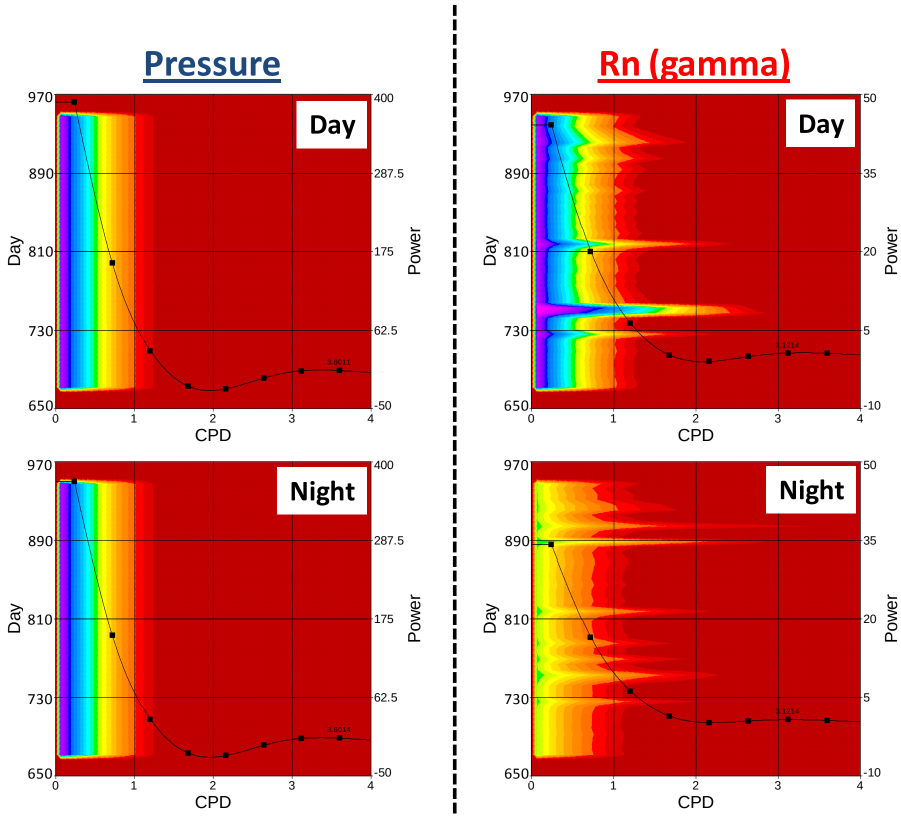

Fig. 12. CWT analysis of the site air pressure time series (left) and the normalized gamma-ray time series (right) decomposed to Day-time and Night-time measurements. Very similar patterns are obtained for pressure and significantly different patterns are observed for radon.

SED
4, 1511–1544, 2012

Influence of a component of solar irradiance on radon signals at 1 km depth

G. Steinitz et al.

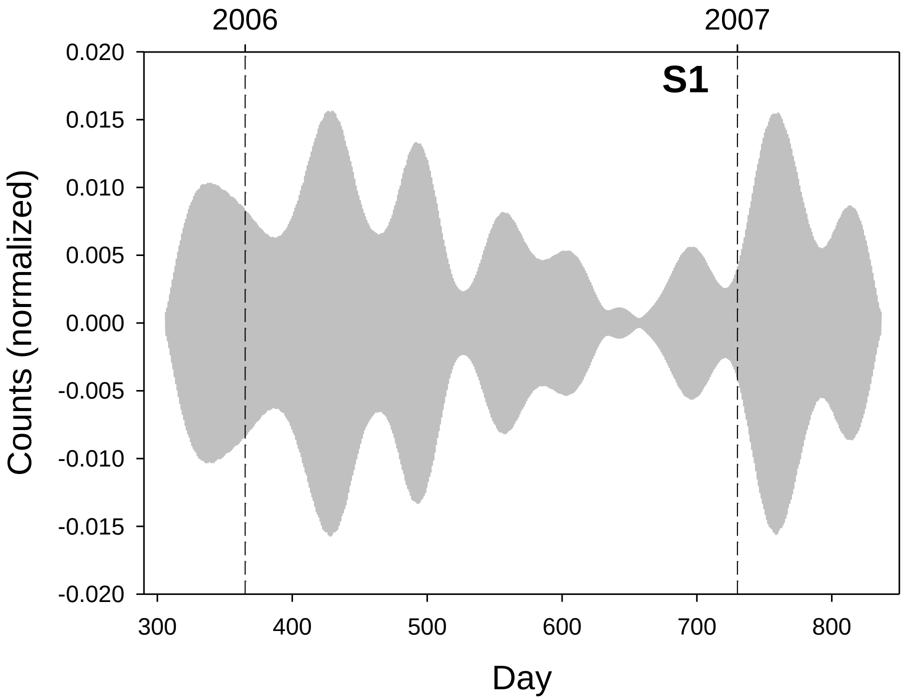

Fig. 13. Time series of the reconstructed 24-h (S1) periodic component in the time series of the gamma measurements (hour averages; normalized). The reconstruction is calculated using an FFT filter of 0.98 to 1.02 CPD (see Fig. 7).

SED
4, 1511–1544, 2012

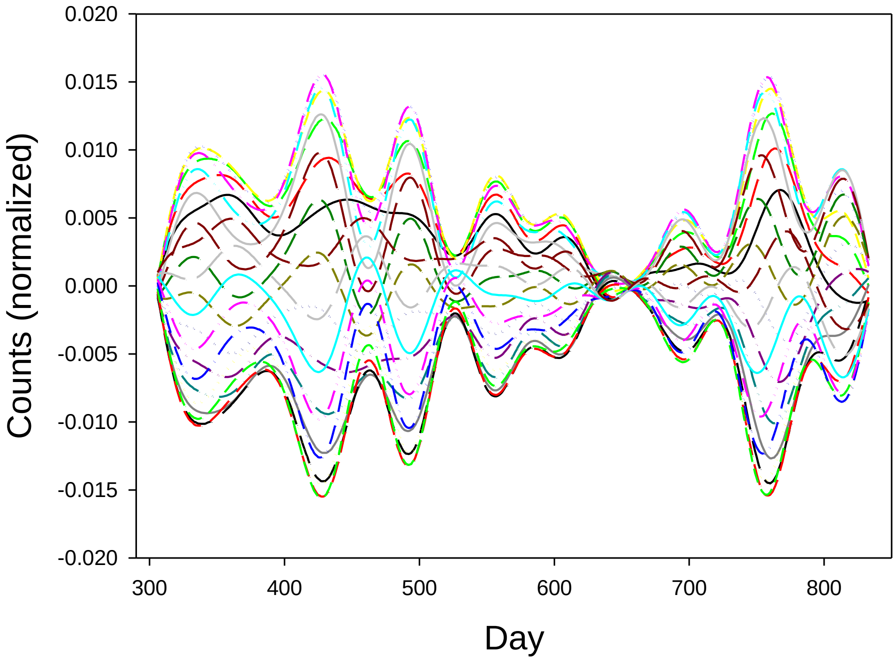

Fig. 14. Plot of reconstructed (FFT) 24-h periodic component decomposed into 24 HID time series. A systematic interwoven pattern is obtained.

SED
4, 1511–1544, 2012

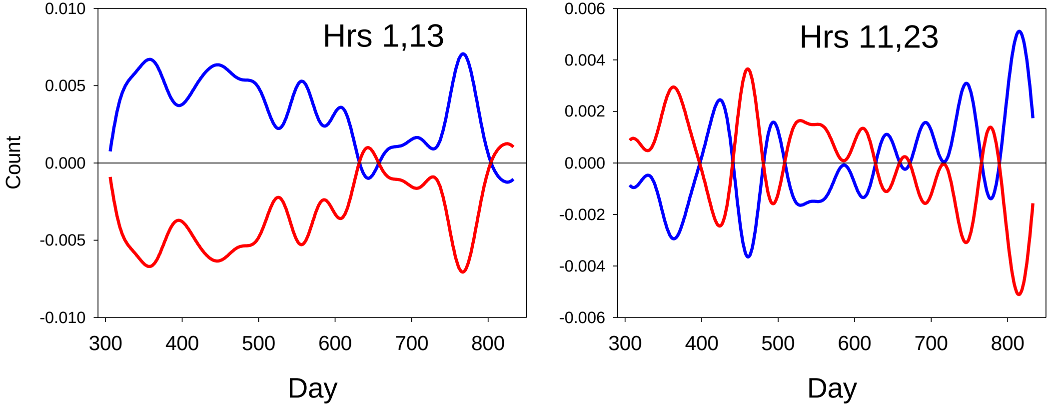

Fig. 15. Two pairs of HID time series separated by 12 h demonstrating inverse temporal patterns.

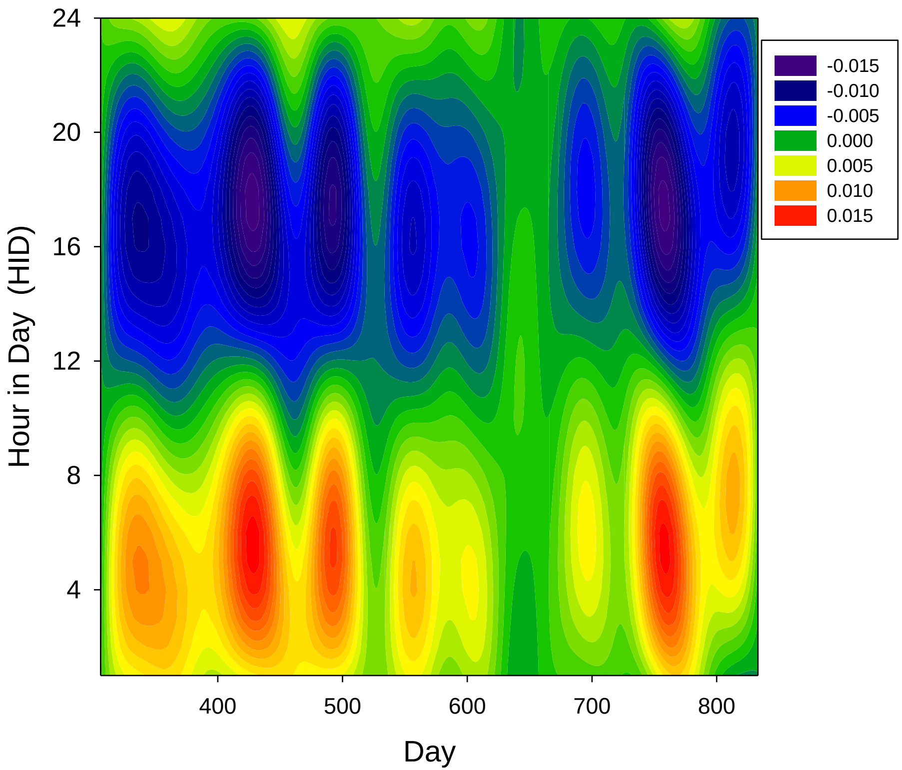

Fig. 16. The variation of the Hourly values of the 24-h periodic component (S1) in a 3-D presentation. X-axis: temporal dimension. Y-axis: Hour in Day. Z-axis: reconstructed (FFT) normalized value. A prominent 12-h asymmetry is indicated throughout. See text.

SED
4, 1511–1544, 2012